

MILITARY ID TAG 5668-MXX-1008-1 - ZN PB ALLOY - MODERN TIMES - FRANCE

Artefact name	Military ID tag 5668-MXX-1008-1
Authors	Christian. Degriigny (HE-Arc CR, Neuchâtel, Neuchâtel, Switzerland) & Marie-Jeanne. Scholl (HE-Arc CR, Neuchâtel, Neuchâtel, Switzerland) & Valentin. Boissonnas (HE-Arc CR, Neuchâtel, Neuchâtel, Switzerland)
Url	/artefacts/921/

✶ The object



Fig. 1: German military ID tag from First World War, recto and verso, 2013,

Credit HE-Arc CR, M-J.Scholl.

✶ Description and visual observation

Description of the artefact	Fragments from an oval shaped German military plate with two circular holes at the central upper edge (Fig. 1). The plate is covered with sediments. Dimensions (70 x 50 mm initially): L = 65mm; W = 50mm; T = 1 mm; WT = 6.3g.
Type of artefact	Military object
Origin	German army, 94th Infantry Regiment, 1918, Carspach, Alsace, France
Recovering date	Recovered in 2011
Chronology category	Modern Times
chronology tpq	1915 A.D. ▼
chronology taq	1915 A.D. ▼
Chronology comment	First World War
Burial conditions / environment	Soil

Artefact location	Pôle d'Archéologie Interdépartemental Rhénan, Sélestat, Alsace
Owner	Pôle d'Archéologie Interdépartemental Rhénan, Sélestat, Alsace
Inv. number	5668-MXX-1008-1
Recorded conservation data	N/A

Complementary information

Information concerning the soldier were given in the centre of the plate. This 1915 model is the oldest standardized model (Directive 594 of the Ministry of War referenced 1085/7.15.B3). Burial conditions (loess sediments, collapsed shelter (Killianstollen) in March 1918 after a French bombing buried the tag at a depth between 3.5 and 6 meters).

Study area(s)

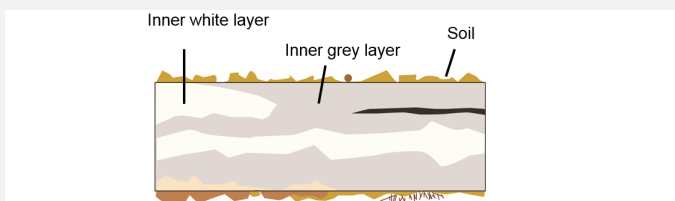


Fig. 2: Location of sample (from fragment b),

Credit HE-Arc CR, M-J.Scholl.

Binocular observation and representation of the corrosion structure

The schematic representation below gives an overview of the corrosion layers encountered on the military tag from a first visual macroscopic observation.



Soil: fine sand (10%), silt (75%), clay (15%), vegetal remains and elements from the corpse (hairs, tissue fibres)

Inner layer grey: translucent and compact, heavily cracked

Inner layer white: opaque and powdery heap, heavily cracked

Credit HE-Arc CR, M-J.Scholl.

Fig. 3: Stratigraphic representation of fragment b of the military tag by macroscopic observation,

MiCorr stratigraphy(ies) – Bi

Sample(s)

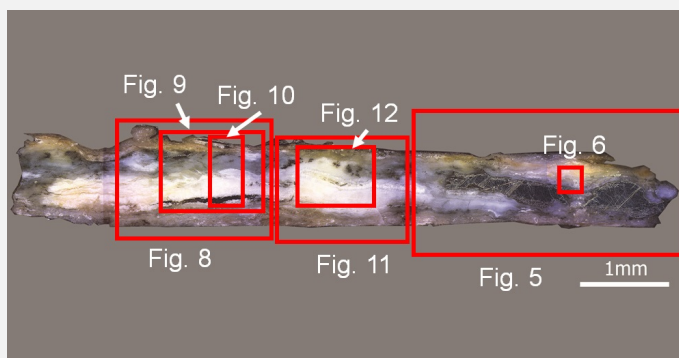


Fig. 4: Micrograph of the cross-section of fragment b of the military tag showing the location of Figs. 5, 6 and 8 to 12. Unetched, dark field, 50x,

Credit HE-Arc CR.

Description of sample

This sample was cut out of fragment b in Fig. 1. The cross-section shows the entire thickness of the plate (L = 8 mm, W = 1 mm). The corrosion goes through the whole metal thickness but a metallic core remains (Figs. 4 and 5).

Alloy

Zn Pb Alloy

Technology

Cold worked (laminated)

Lab number of sample

None

Sample location

HE-Arc CR, Neuchâtel, Neuchâtel

Responsible institution

Pôle d'Archéologie Interdépartemental Rhénan, Sélestat, Alsace

Date and aim of sampling

2013, metallography and chemical analyses

Complementary information

None.

Analyses and results

Analyses performed:

Metallography (etched with HCl 10 M reagent), XRF, SEM/EDS, FTIR and Raman spectroscopy.

Non invasive analysis

None.

Metal

The remaining metal is a zinc alloy (Table 1) containing 1.8% in weight lead. Lead appears in the metal in the form of small flattened white Pb inclusions (Fig. 6), confirming the manufacturing technique, namely lamination. The etched metal does not show any specific microstructure (Fig. 7).

Elements	Zn	Pb
mass%	98.2	1.8

Table 1: Chemical composition of the metal. Method of analysis: SEM-EDS, Lab of Electronic Microscopy and Microanalysis, IMA (Néode), HEI Arc.

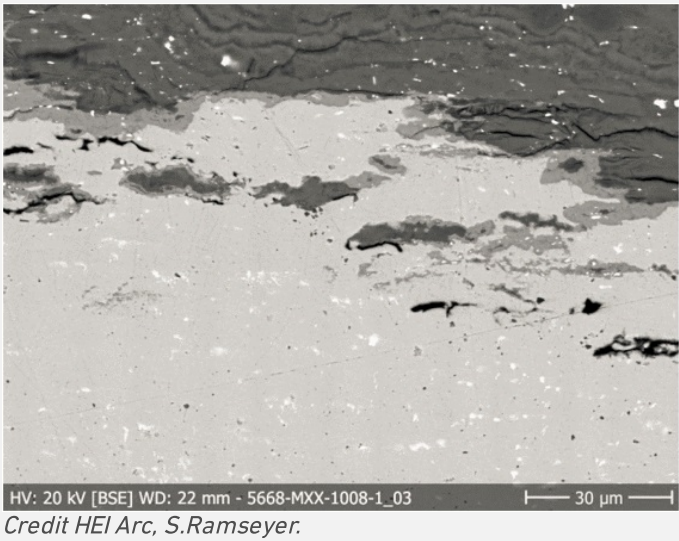
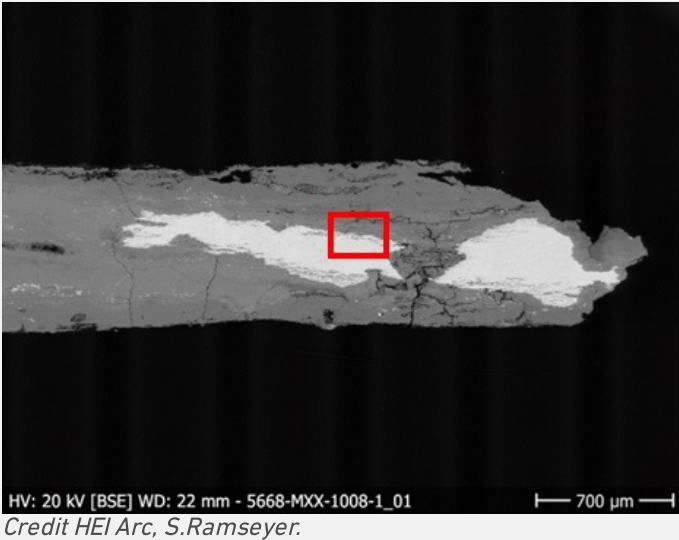
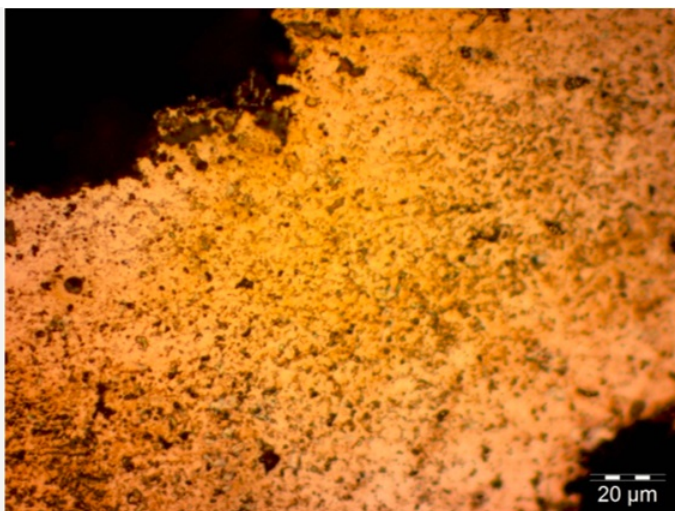


Fig. 7: Micrograph of the cross-section, etched, bright field, 500x,



Credit HE-Arc CR.

Microstructure	Unknown
First metal element	Zn
Other metal elements	Pb

Complementary information

None.

✧ Corrosion layers

The corrosion spreads on the entire thickness of the plate and different forms of corrosion within the same plate have occurred (multiform corrosion). Sometimes the metal core still remains, sometimes not.

The corrosion structure is multi-layered: several corrosion products overlap. However they are not all continuous layers, since some of them are isolated. Most of the corrosion products layers show structural voids (up to 100 μm thick) and some cracks inside. Three layers can be distinguished (Fig 8 and Figs. 16 or 17 - only Fig. 16 is detailed below) which have the same elements but in different proportions (Figs. 9, 10 and table 2):

- Inner grey layer – CP1 (up to 1 mm thick) is a translucent, compact layer and constitutes most part of the corrosion products. Corroded metal appears inside this layer rich in Zn and O (Table 2) as lead inclusions within a black corrosion product (Figs. 8 and 10). Sulphur has also been detected by SEM-EDS inside this layer, near the surface, where the colour turns into grey-orange (zinc sulfide or sulphates but to be confirmed, table 2).
- Inner white layer – CP2 (up to 0.6 mm thick) is an opaque and powdery heap, occurring in different places inside inner grey layer and sometimes near the surface, as pitting corrosion. The interface between inner layers grey and white is gradual. Localized aggregates showing a crystalline microstructure of thickness of 50 μm are located against the walls of a structural void, inside the white corrosion product (Figs. 11 and 12).
- Inner black layer – CP3 (up to 0.1 mm) is an opaque and compact layer with a composition similar to inner white layer (Table 2).

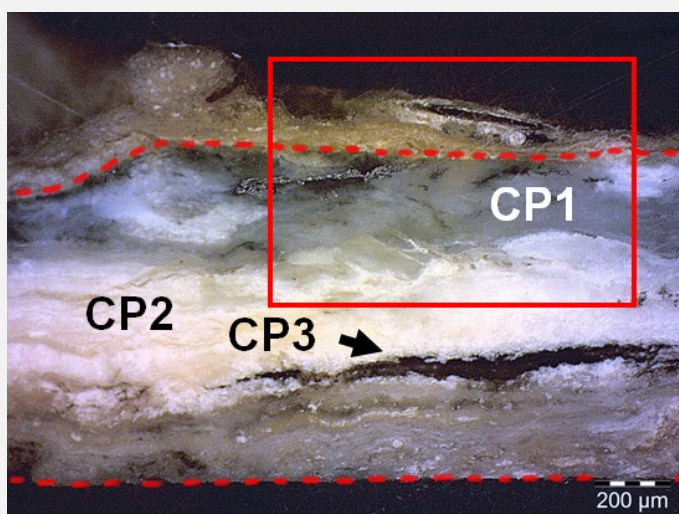
On top the metal is covered with non-metallic materials (NMM1, fine sand (10%), silt (75%), clay (15%), vegetal remains) and elements from the corpse (hairs, tissue fibers)). An outer corrosion product has not been identified, but may occur, because zinc combined with sulphur was detected at the surface (Table 2).

The inner grey layer (CP1, Figs. 8 and 16) has been identified by FTIR as a zinc carbonate (smithsonite), mixed with other unidentified corrosion products. Raman spectra seems to confirm it (Fig. 13). The exact composition of the inner white layer (CP2) is unknown. It shows a bluish fluorescence under UV light and has been identified by FTIR as a mixture of zinc oxides and carbonates, that could be zinc hydroxycarbonates (hydrozincite). Raman spectroscopy shows also a mixture of carbonates and other corrosion products (Fig. 14). The inner black layer (CP3) is a zinc carbonate as well, identified by FTIR and Raman spectroscopy (Fig. 15) appearing as a vein between layers of grey and white (Fig. 8).

Elements	O	Zn	Pb	S
----------	---	----	----	---

Inner grey layer (CP1)	++	+++	+	
Black inclusions		+	+++	
Inner white layer (CP2)	++	+++	+	
Inner black layer (CP3)	++	+++	+	
Inner grey-orange layer	+	++		++
Remnant metal phase		+++	+	

Table 2: Chemical composition of the different corrosion layers from Fig. 10. Method of analysis: SEM-EDS, Lab of Electronic Microscopy and Microanalysis, IMA (Néode) (+++: high concentration, ++ medium concentration, + low concentration, nd: not-detected).



Credit HE-Arc CR.

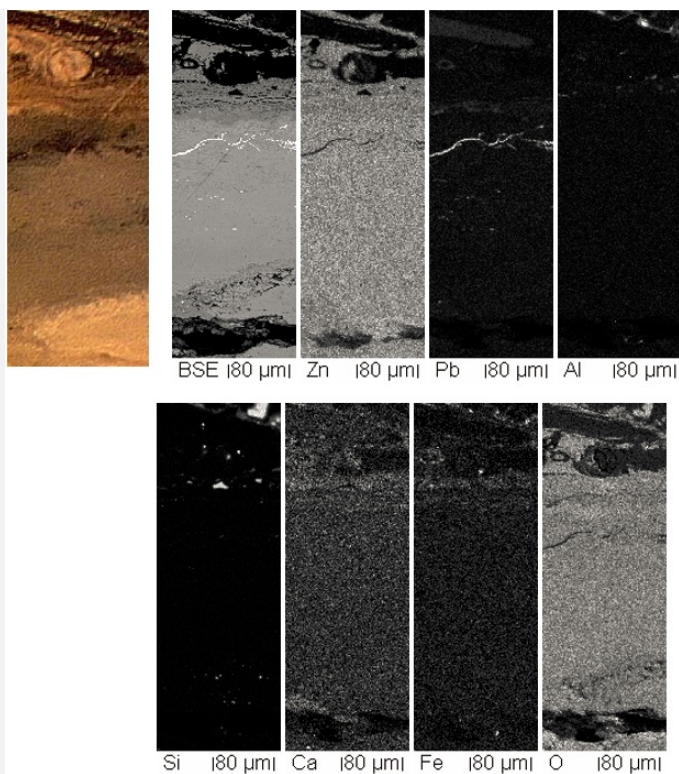
Fig. 8: Micrograph of the cross-section, from Fig. 4 (detail) and corresponding to the stratigraphy of Fig. 5, unetched, dark field, 50x. View of the inner layers and the limit of the original surface (red line). We can see that the interfaces between the different layers are not well defined: some of the white corrosion product is found inside the inner grey layer. The micrograph of Fig. 9 is marked by a rectangle,



Credit HEI Arc, S.Ramseyer.

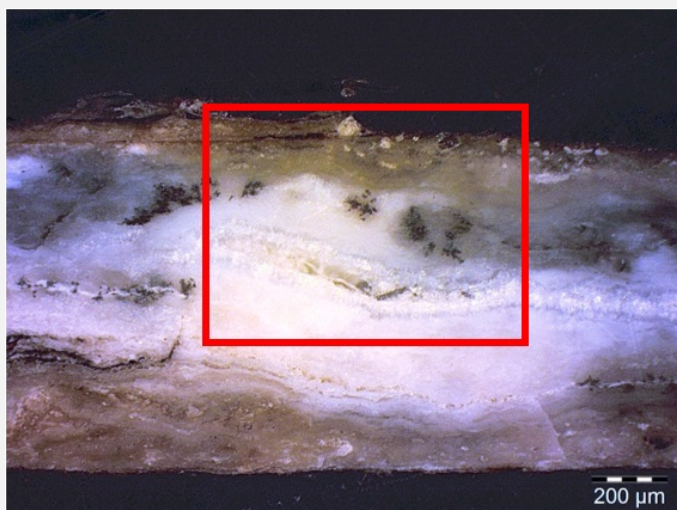
Fig. 9: SEM image of the cross-section from Fig. 8 (detail), BSE-mode. The area selected for elemental chemical distribution (Fig. 10) is marked by a rectangle,

Fig. 10: SEM image of the cross-section from Fig. 9 (detail), SE-mode, and elemental chemical distribution. Method of examination: SEM/EDS, Lab of Electronic Microscopy and microanalysis, IMA (Néode), HEI Arc,



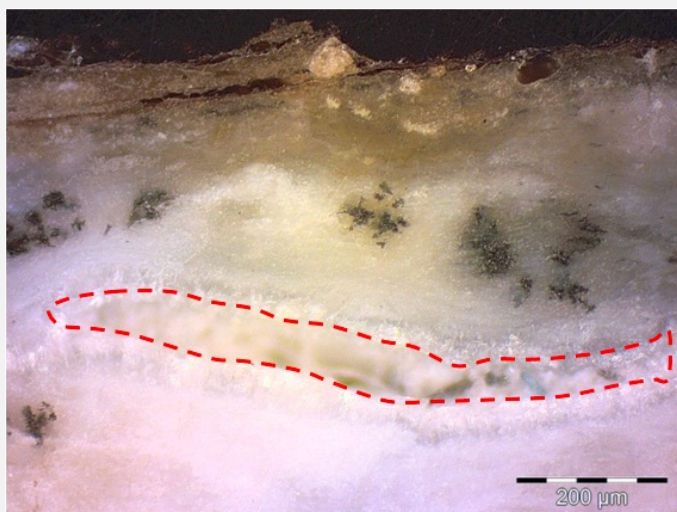
Credit HEI Arc, S.Ramseyer.

Fig. 11: Micrograph of the cross-section, from Fig. 4 (detail), unetched, dark field, 50x. The micrograph of Fig. 12 is marked by a rectangular,



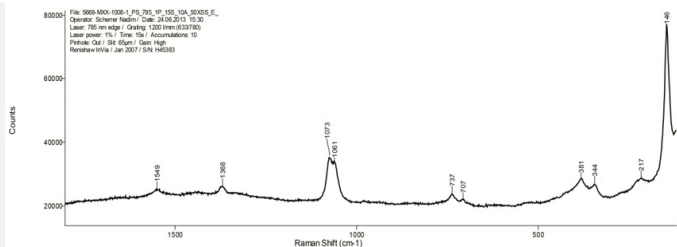
Credit HE-Arc CR.

Fig. 12: Micrograph of the cross-section, from Fig. 9 (detail) unetched, dark field, 100x. Structural void (dotted red line) with aggregates,

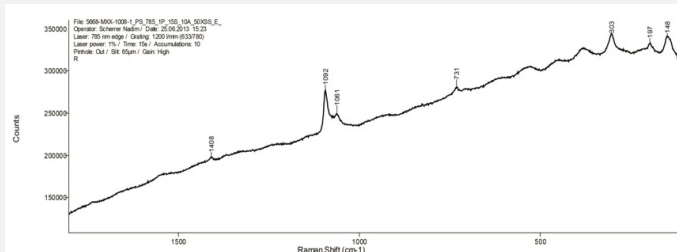


Credit HE-Arc CR.

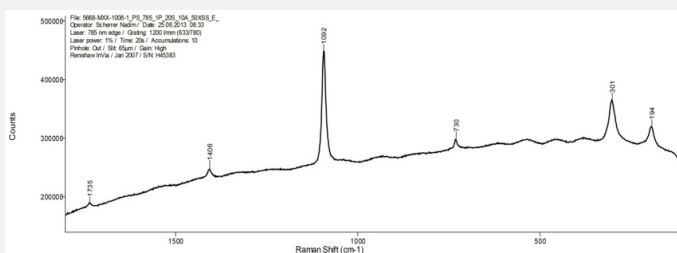
Fig. 13: Raman spectrum of the inner grey layer (CP1 on Fig. 8, ZnCO_3 – smithsonite?). Settings: laser wavelength 532nm,



Credit HKB.



Credit HKB.



Credit HKB.

acquisition time 10s, one accumulation, filter D2 (0.75-0.8mW), hole 500, slit 80, grating 600. Method of analysis: Raman spectroscopy, Art Technological Laboratory, Departement Conservation HKB,

Fig. 14: Raman spectrum of the inner white layer (CP2 on Fig. 8, zinc hydroxycarbonate?). Settings: laser wavelength 532nm, acquisition time 10s, one accumulation, filter D2 (0.75-0.8mW), hole 500, slit 80, grating 600. Method of analysis: Raman spectroscopy, Art Technological Laboratory, Departement Conservation HKB,

Fig. 15: Raman spectrum of the inner black layer (CP3 on Fig. 8, zinc carbonate?). Settings: laser wavelength 532nm, acquisition time 10s, one accumulation, filter D2 (0.75-0.8mW), hole 500, slit 80, grating 600. Method of analysis: Raman spectroscopy, Art Technological Laboratory, Departement Conservation HKB,

Corrosion form Multiform - transgranular

Corrosion type Unknown

Complementary information

None.

✧ MiCorr stratigraphy(ies) – CS

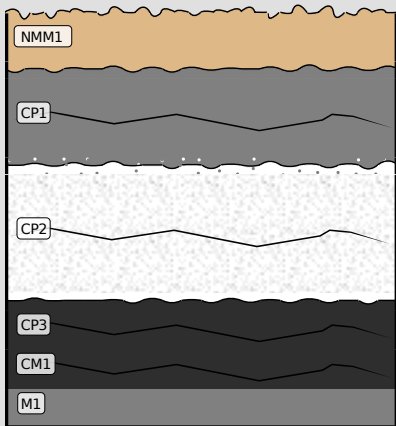
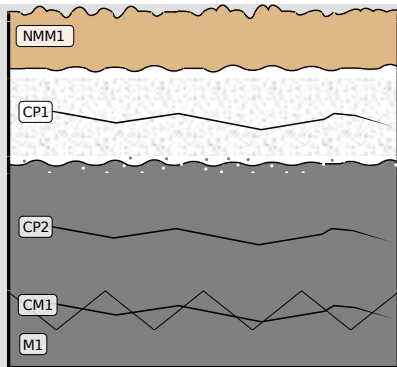


Fig. 16: Stratigraphic representation of fragment b of the military tag in cross-section (dark field) using the MiCorr application. The characteristics of the strata are only accessible by clicking on the drawing that redirects you to the search tool by stratigraphy representation. This representation can be compared to Fig. 10, Credit HE-Arc CR, M-J.Scholl.

Fig. 17: Stratigraphic representation of fragment b of the military tag in cross-section (dark field) using the MiCorr application. The characteristics of the strata are only accessible by clicking on the drawing that redirects you to the search tool by stratigraphy representation. This



representation is different from Fig. 10 due to the inversion of CP1 and CP2. Furthermore, CP3 is not represented, Credit HE-Arc CR, M-J.Scholl.

✧ Synthesis of the binocular / cross-section examination of the corrosion structure

The schematic representation of corrosion layers of Fig. 3 integrating additional information based on the analyses carried out is given in Fig. 18.

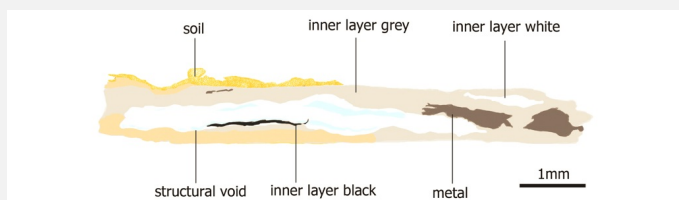


Fig. 18: Improved representation of the stratigraphy of corrosion layers of the military tag from visual observations and analyses,

Strate	Composition
Soil (S)	Elements from soil, organic elements
Grey corrosion product (CP1)	Zinc carbonate (smithsonite) + S
White corrosion product (CP2)	Zinc hydroxycarbonate + mixture of CP
Black corrosion product (CP3)	Zinc carbonate
Corroded metal (CM)	
Metal (M)	Zn-Pb

Credit HE-Arc CR, M-J.Scholl.

✧ Conclusion

The military tag is made of a laminated sheet of zinc-lead alloy. The corrosion has entirely penetrated the objet leaving though some spots of remaining original metal inside the corrosion products. Lead particles are not affected by the corrosion process. The main corrosion products are zinc carbonates (smithsonite) and hydroxycarbonates (hydrozincite) but mixtures of different corrosion products can occur. These corrosion products are intermixed and heavily cracked.

✧ References

References on object and sample

Reference object

1. Scholl, M-J. (2013) Caractérisation des plaques d'identification militaires en zinc provenant du site de Carspach (Alsace, Haut-Rhin, F). Travail de Bachelor Filière Conservation-restauration, Haute Ecole Arc de Conservation-restauration, Neuchâtel.

Reference sample

2. Scholl, M-J. (2013) Caractérisation des plaques d'identification militaires en zinc provenant du site de

References on analytic methods and interpretation

3. Moser, Z. et al. (1994) The Pb-Zn (Lead-Zinc) System. In Journal of Phase Equilibria, vol.15, n°6, p.643-644.
4. Goodwin, F. E. (2010) "Corrosion of Zinc and its Alloys". In Cottis, R. A. Shreir's corrosion. vol.3 Corrosion and degradation of engineering materials. Elsevier Science, Oxford, 2078-2093.
5. De Zoubov, N. et Pourbaix, M. (1963) « Zinc », In Pourbaix, Marcel. Atlas d'équilibres électrochimiques. Gauthier-Villars, Paris, 406-413.